

Detection of Pathogenic Biofilms with Bacterial Amyloid Targeting Fluorescent Probe, CDy11

Jun-Young Kim,^{†,‡,§} Srikanta Sahu,[§] Yin-Hoe Yau,^{||} Xu Wang,[†] Susana Geifman Shochat,^{||} Per Halkjær Nielsen,^{‡,⊥} Morten Simonsen Dueholm,[⊥] Daniel E. Otzen,[#] Jungyeol Lee,[†] May Margarette Salido Delos Santos,[‡] Joey Kuok Hoong Yam,^{‡,∇} Nam-Young Kang,[§] Sung-Jin Park,[§] Hawyoung Kwon,^{†,‡} Thomas Seviour,[‡] Liang Yang,^{‡,||} Michael Givskov,^{‡,¶} and Young-Tae Chang^{*,†,§}

[†]Department of Chemistry & Med Chem Program, Life Sciences Institute, National University of Singapore, 3 Science Drive 3, 117543, Singapore

[‡]Singapore Centre on Environmental Life Science Engineering (SCELSE), Nanyang Technological University, 637551, Singapore

[§]Singapore Bioimaging Consortium, Agency for Science, Technology and Research, 11 Biopolis Way, # 02-02 Helios, 138667, Singapore

^{||}School of Biological Sciences, Nanyang Technological University, SBS-04s-43, 60 Nanyang Avenue, 637551, Singapore

[⊥]Center for Microbial Communities, Department of Chemistry and Bioscience, Aalborg University, Fredrik Bajers Vej 7H, 9220 Aalborg, Denmark

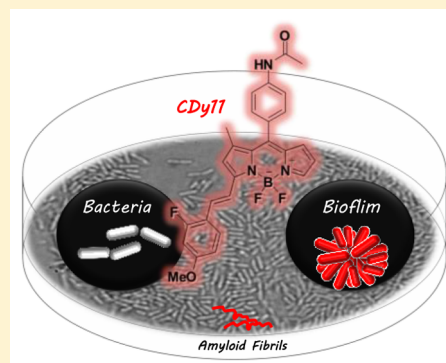
[#]Interdisciplinary Nanoscience Center (iNANO), Department of Molecular Biology and Genetics, Aarhus University, 8000 Aarhus C, Denmark

[∇]Interdisciplinary Graduate School, Nanyang Technological University, 637551, Singapore

[¶]Costerton Biofilm Center, Department of Immunology and Microbiology, Faculty of Health and Medical Sciences, University of Copenhagen, Blegdamsvej 3B, DK-2200 Copenhagen, Denmark

Supporting Information

ABSTRACT: Bacterial biofilms are responsible for a wide range of persistent infections. In the clinic, diagnosis of biofilm-associated infections relies heavily on culturing methods, which fail to detect nonculturable bacteria. Identification of novel fluorescent probes for biofilm imaging will greatly facilitate diagnosis of pathogenic bacterial infection. Herein, we report a novel fluorescent probe, CDy11 (compound of designation yellow 11), which targets amyloid in the *Pseudomonas aeruginosa* biofilm matrix through a diversity oriented fluorescent library approach (DOFLA). CDy11 was further demonstrated for in vivo imaging of *P. aeruginosa* in implant and corneal infection mice models.



INTRODUCTION

Despite the discovery of antibiotics, bacterial infections remain as one of the major threats to the human society. This is partly caused by dissemination of resistance toward the current assortment of antibiotics and an almost 30 year discovery void of new classes of antimicrobial drugs.¹ Another important cause of antibiotic resistance and persistent infections is the capability of bacteria to form biofilms. Microorganisms are able to form surface-attached multicellular biofilm communities as a dominant lifestyle in nature.² These densely populated communities are encased in large amount of self-generated extracellular polymeric substances (EPS). The thick EPS matrix offers protection to the biofilm cells against otherwise harmful conditions, such as oxidative stress, extreme pH change and high dose of antibiotics. Biofilms are up to 1000 times more

resistant to antibiotics than their free-living counterparts.³ What is more, biofilms are able to survive and evade host immunity.^{4,5} According to the National Institute of Health, more than 80% of all infections are associated with biofilms.⁶ Furthermore, biofilm bacteria are able to disperse and spread to new areas.⁷ Bacteria in biofilm-associated infections often appear non-culturable.⁸ Therefore, rapid and reliable identification of biofilm-associated infections are important for choosing the proper treatment strategy in the clinics, such as antimicrobial administration or surgical removal of the infected tissue.

Biofilm EPS mainly consists of extracellular DNA, proteins and polysaccharides. Several compounds have been reported to

Received: November 5, 2015

Published: December 18, 2015

specifically label EPS components. For example, DNA staining dyes such as ethidium bromide, Syto9 or DAPI are frequently used to localize extracellular DNA in biofilms.⁹ Hippastrum Hybrid (Amaryllis) Lectin, HHA, that specifically binds to either 1,3- or 1,6-linked mannosyl units in polysaccharides is used for biofilm detection after conjugating with fluorophore due to its binding specificity with Psl polysaccharide, a key component of *P. aeruginosa* biofilms.¹⁰

Recently, ligand targeted ultrasound contrast agents (UCAs) were reported to detect biofilm *in vitro* under high-frequency scanning acoustic microscopy.¹¹ Even though it showed the possibility as a biofilm detecting tool of application, there is no established method for *in vivo* biofilm imaging so far.

We previously developed various imaging probes and sensors for stem cells,¹² pancreatic alpha cells,^{13,14} beta cells,¹⁵ and neuron¹⁶ by screening our in house diversity oriented fluorescent library (DOFL).¹⁷ To develop clinically relevant biofilm imaging probes, *P. aeruginosa* was chosen, as the bacterium is a well-known opportunistic pathogen, associated with cystic fibrosis of hospitalized patients with immune-compromised conditions,¹⁸ and commonly found in catheters¹⁹ and in contact lens.²⁰ In this study, Functional amyloids in *Pseudomonas* (Fap) was chosen as the molecular target (biomarker) of the fluorescent probe, due to its importance for *Pseudomonas* biofilm structure and function.^{21–23}

RESULTS

Discovery of CDy11. Thousands of DOFL compounds¹⁷ were screened in two different *P. aeruginosa* strains, PAO1 wild type and PAO1Δfap, which lack the complete fap operon, required for Fap biogenesis.^{24,25} The primary screening was performed in 96 well format with the two strains of bacteria culture, and the relative fluorescence intensity was compared under EVOS portable fluorescent microscope. Dyes with stronger signal to PAO1 wild types were selected as primary hits. Then, secondary and tertiary screenings were carried out by testing all of the primary hit candidates with more advanced model of cover-glass slide biofilms cultivated in 50 mL conical tubes (Figure 1A).

Images were acquired after 1 h of incubation of dye compounds with biofilms. The images were then analyzed based on fluorescence intensity from two different samples of the PAO1 and PAO1Δfap biofilms. Based on the clear distinction of the fluorescence images and reproducibility of the results, the best compound was selected and named as CDy11 (Scheme 1). CDy11 shows strong selective staining in PAO1 biofilms compared to those of PAO1Δfap biofilms (Figure 1B) and of planktonic cells PAO1 (Supporting Information Figure S1).

To investigate the generality of CDy11 for other bacterial amyloid of biofilm, we also tested two other species of bacteria, *E. coli* and *S. typhimurium* in addition to *P. aeruginosa*. Apparently, amyloid expressing wild type bacteria showed much stronger staining by CDy11 in comparison to amyloid deficient mutant, demonstrating the general applicability of CDy11 to broad range of bacterial biofilm detection (Supporting Information S2).

The sensitivity of CDy11 has also been measured by *in vitro* fluorescence response assay with serial dilution of bacteria in biofilm, showing the apparent detection limit of 8×10^8 CFU/mL (Supporting Information S3).

We further analyzed the staining pattern of CDy11 in biofilms with structure illuminated microscope. Biofilms were

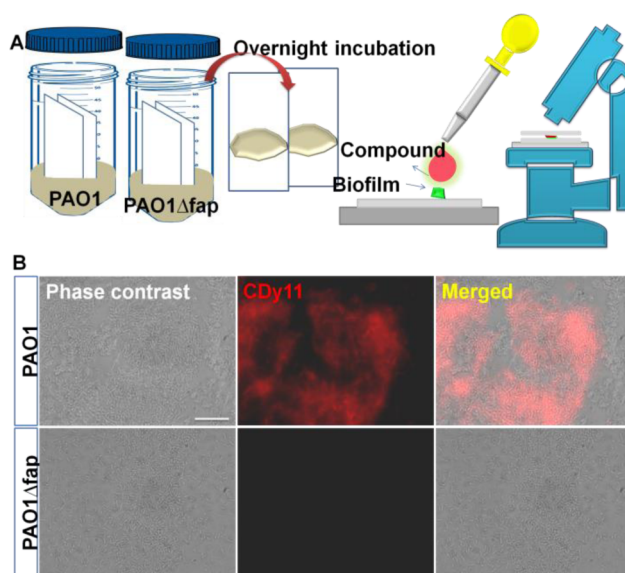
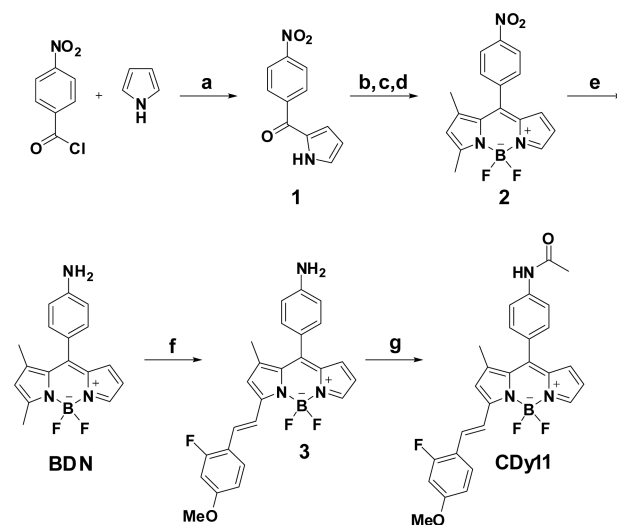


Figure 1. Established screening format. CDy11 which was developed as a bioimaging probe with established screening format. It was targeted PAO1 biofilms specifically. (A) Screening format for finalizing primary hit candidates from 96 well plate based screening. Primary hits were applied biofilms on cover glass for 1 h and images are taken under fluorescence microscope. (B) Phase contrast and fluorescent images acquired from CDy11 treated PAO1 biofilms and PAO1Δfap biofilms. Scale bar, 10 μm .

Scheme 1. Synthesis of CDy11^a



^a(a) MeMgBr, THF, -78 °C to RT, overnight; (b) NaBH₄, THF/H₂O (10:1), 0 °C to RT, 2 h; (c) 2,4-dimethyl pyrrole, InCl₃, CH₂Cl₂, RT, 3 h; (d) i. DDQ, CH₂Cl₂, RT, 15 min, ii. BF₃·Et₂O, Et₃N, 0 °C to RT, 8 h; (e) Pd/C, hydrazine monohydrate, EtOH, reflux, 2 h; (f) 2-Fluoro-4-methoxybenzaldehyde, pyrrolidine, MeCN, 85 °C, 5 min; (g) AcCl, NaHCO₃, CH₂Cl₂, 0 °C to RT, 30 min.

cultivated in 8 well chamber plates by incubating PAO1-GFP strain with ABTGC media for 16 h at 37 °C incubator. Biofilms were exposed to 1 μM of CDy11 for 1 h before acquiring images. The GFP signal allowed for observation of distribution of individual bacterial cells in the biofilms and the CDy11 signal was recorded using the TRITC (Tetramethylrhodamine) channel. Two 3D-SIM images were acquired at two different fluorescent channels and merged. The signal from CDy11 was

observed outside of cells (Figure 2, merged). The PAO1 biofilms showed much stronger staining intensity than the

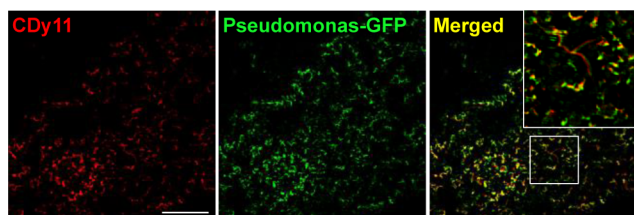


Figure 2. Super resolution images of biofilms incubated with CDy11. Images of CDy11 stained PAO1-GFP biofilms acquired on a structure illuminated microscope using a $\times 100$ objective oil lens. The merged image shows that fluorescent signal of CDy11 overlapped with GFP signal of PAO1-GFP biofilms. Image in white rectangle was magnified to show localization of CDy11. Scale bar, 10 μm .

PAO1 Δ fap biofilms, suggesting that the putative binding target of CDy11 was Fap or Fap conjugated components of the biofilm.

Validation of the CDy11 Binding Target. To prove that Fap was the binding target of CDy11, *P. aeruginosa* Fap was produced and purified from *E. coli* by expressing the Fap operon from *P. aeruginosa*. Purified Fap fibril structure was verified under transmission electron microscopy (Figure 3A),

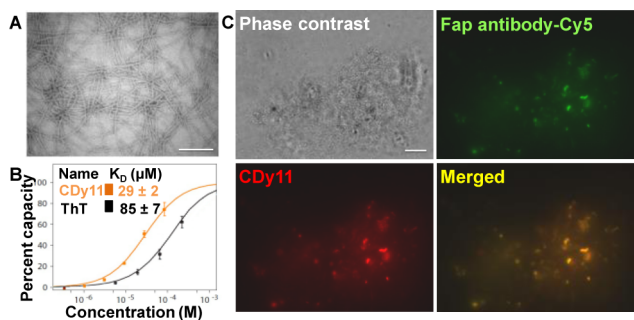


Figure 3. Evaluation of target of CDy11. (A) Transmission electron microscopic image of purified amyloid. Scale bar, 400 nm. (B) Surface plasma resonance assay with CDy11 and purified amyloid after immobilization on chips. Values were calculated by measurements for their response unit by flowing ThT and CDy11. (C) Co-localization of CDy11 and Fap antibody. Biofilms were incubated with primary Fap antibody and secondary antibody linked with Cy5. Subsequently, CDy11 was treated for 1 h before acquiring images. The images were captured using a fluorescence microscope equipped with $\times 100$ objective lens. Scale bars, 10 μm . The images are shown in pseudocolors.

before immobilization by an amine coupling reaction on a CMS sensor chip for a binding assay using a Biacore surface plasmon resonance biosensor. Thioflavin-T, which is widely used for amyloid studies, was chosen as a positive control. The binding constant (K_D) for Thioflavin T was $85 \pm 7 \mu\text{M}$ (Figure 3B). CDy11 had >2 times higher binding affinity (K_D $29 \pm 2 \mu\text{M}$) than Thioflavin T. Finally, expression of the Fap subunit protein was checked with Fap antibodies and CDy11 in PAO1 biofilms. Antiserum raised against the Fap amyloid protein from *P. aeruginosa* was incubated with biofilms for 2 h at 37 $^\circ\text{C}$, then Cy5-linked secondary antibody was incubated for 1 h, before treatment of 1 μM of CDy11. Each fluorescence signal was obtained either with a TRITC filter or a Cy5 filter under a fluorescence microscope (Figure 3C). For the specificity test of

CDy11 to the amyloid, the colocalization of CDy11 and Fap antibody staining was analyzed by image comparison and high Pearson's coefficient of 0.91 was observed (Supporting Information S4). On the basis of these data, we conclude that CDy11 specifically binds to Fap and not to other cellular components.

Application of CDy11 in an Animal Model of Infection. In general, *P. aeruginosa* is usually present in the lungs of cystic fibrosis patients but also, in the inserted part of catheters removed by surgery¹⁹ and in contact lenses.²⁰ To investigate the feasibility of CDy11 application for detecting in vivo biofilms, a corneal infection model was generated in mice.²⁶ Black mice were anesthetized by injection with ketamine/xylazine into peritoneal cavity and their cornea scratched with a blade (Figure 4A). To generate an eye infection, the GFP-tagged *P. aeruginosa* (PAO1-GFP) suspended in PBS buffer (1–2 μL , $5 \times 10^7 \sim 10^8$ CFU) was dropped in the eyes and mice were maintained for 2 days. GFP signal was traced at different time points post infection to confirm the propagation of the *P. aeruginosa* infection in the cornea. GFP signals could be detected within the infected mouse cornea at 12 h post infection and appeared fully saturated at 36 h post infection (Supporting Information Figure S5).

CDy11 was tested using this corneal infection model after 24 h's infection with PAO1-GFP. First, all images from the control scratched eyes and *P. aeruginosa* infected eyes were acquired without CDy11 treatment. As a result, only the GFP signal was detected in bacterial infection eye. Subsequently, 5 μM of CDy11 was dropped in both eyes and incubated for 10 min where after the eyes were briefly washed with PBS buffer prior to acquiring images. While there was no obvious fluorescent signal from CDy11 in the control eye (Figure 4B (–)CDy11), clear fluorescence signals were detected in the infected eye (Figure 4B (+)CDy11). This observation revealed that the propagated *P. aeruginosa* biofilms could be detected in vivo by simple dropping of CDy11 without any surgical or culture process. Also, retention time of CDy11 on eye was investigated in a time dependent manner by acquiring images under stereomicroscope. The fluorescence intensity of CDy11 peaked after 10 min incubation and most of the signal was gone within 1 h (Figure 4C, D). Subsequently, eyes were extracted by sacrificing mice after imaging and sectioning samples were prepared to check *P. aeruginosa* infection in corneal regions with Fap antibody. No amyloid signal was observed from control eye by incubating with Fap antibody (Supporting Information Figure S6A), but a clear signal was detected from the *P. aeruginosa* infected eye by Fap antiserum (Supporting Information Figure 6B) and CDy11 signal. The GFP signal from *P. aeruginosa* and Cy5 signal from Fap antibody overlapped well (Figure 4E). Based on immunohistochemical evidence with eye sectioning tissues, we conclude that CDy11 specifically targets biofilm forming regions.

Next, we applied a mouse implant model to test the capacity of CDy11 to detect *P. aeruginosa* biofilms in a surgical format.²⁷ Silicone tubes were precolonized by bacteria and subsequently inserted into the peritoneal cavity 1 day before the experiment. BALB/c mice were assigned to each of the two groups and 100 μM CDy11 (200 μL) was injected into the mice via the peritoneal cavity 2 h before recovering the implants (Supporting Information Figures S7A). As a mock control, a similar volume of buffer was injected into the second set of mice. In addition, CDy11 was injected into a set of mice which

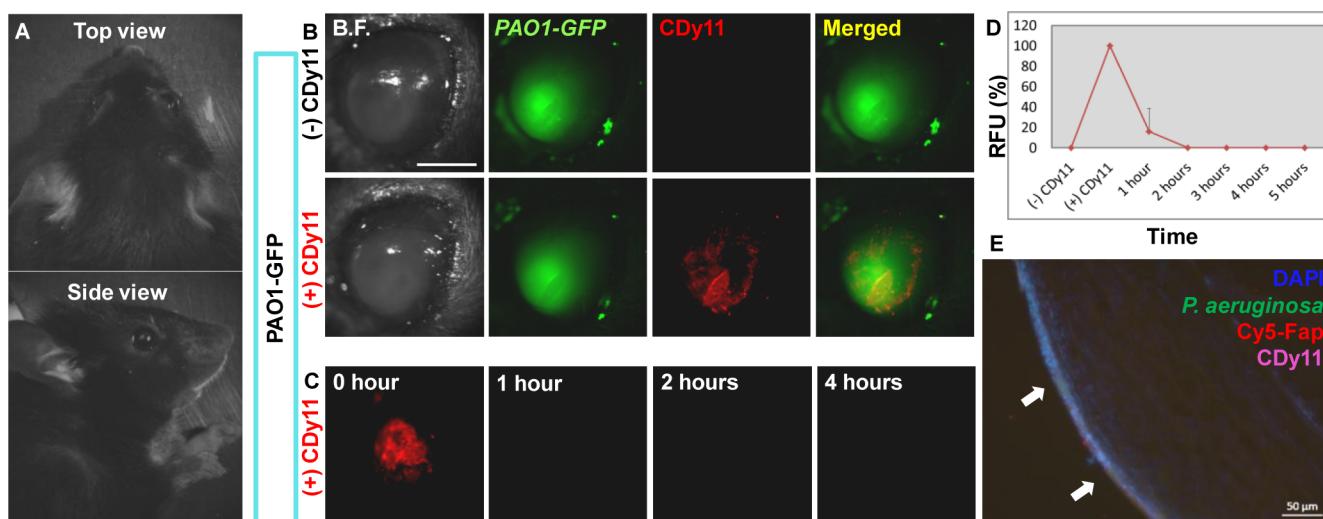


Figure 4. Visualization of *P. aeruginosa* infection by CDy11 in corneal infection model. CDy11 was tested in corneal infection model from mouse which was incubated for 24 h post infection of *P. aeruginosa* (PAO1–GFP). (A) Overview of mouse head which has used for in vivo imaging. (B) In vivo imaging of bacterial infection eye with CDy11. Green fluorescence signals were detected *P. aeruginosa* (PAO1–GFP) infected eye. No signals were detected in *P. aeruginosa* infected eye without CDy11. *P. aeruginosa* infection eye was stained with CDy11. (C) CDy11 signals were gone after 1 h maintenance before imaging under stereomicroscope. (D) Quantification of remaining CDy11 signals in the bacterially infected eye. Fluorescence intensity peaks after 10 min of incubation. (E) Quadruple-fluorescence tissue image with DAPI/GFP/CDy11/Cy5-Fap antibody. White arrows indicate the overlapped signals of Hoechst/PAO1–GFP/Cy5-Fap/CDy11. Scale bars, 2 mm. Overview images were taken under stereomicroscope with $\times 4$ magnification and eye images were taken under stereomicroscope with $\times 34$ magnification.

had been installed with uncolonized silicone tubes in the peritoneal cavity.

All silicone tubes were collected after 2 h incubation to observe CDy11 fluorescence of the inner surface of the silicone tube by means of laser confocal scanning microscopy. As a result, biofilm coated silicone tube using PAO1 Δ fap–gfp²⁴ strain which does not produce Fap in the EPS was not stained by CDy11 (Figure 5A). *P. aeruginosa* biofilm (PAO1–GFP)

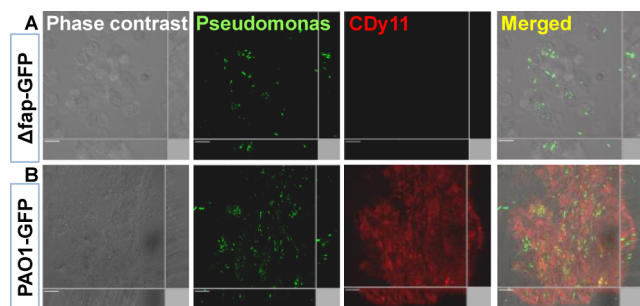


Figure 5. Test of CDy11 in implant model. CLSM images of the *P. aeruginosa* (PAO1–GFP) colonizing silicone implants after removal from BALB/c mice at day 1 after insertion. Green fluorescent areas represent *P. aeruginosa*. Insertion of silicone tube into mice which was precoated with (A) PAO1 Δ fap–GFP and (B) PAO1–GFP biofilms. Images of the microcolonies adhering to the silicone implants with CDy11. Only PAO1–GFP biofilms coated silicone tube was stained by CDy11. Scale bars, 10 μ m.

coated silicone tubes were specifically stained with CDy11 (Figure 5B) while, biofilms under same condition without CDy11 showed only the GFP signal (Supporting Information Figure S7B). The silicone tubes without *P. aeruginosa* precoating were also examined by injection of same amount of CDy11. Immune cells had moved into the silicone tubes but those were not stained by CDy11 (Supporting Information Figure S7B).

In conclusion, CDy11 showed its feasibility as a bioimaging probe for detecting biofilms of *P. aeruginosa* in two different in vivo models of infection.

DISCUSSION

In this paper, we have reported the development of CDy11, a novel bioimaging probe for detecting biofilms based on high throughput cell based screening using the *P. aeruginosa*. SPR data and antibody staining demonstrates that CDy11 binds to *P. aeruginosa* amyloid proteins, one of the key components of biofilms. Bacterial amyloids have important role in attachment of surface and initiation of biofilm formation.^{24,25} Therefore, CDy11 provides an opportunity to investigate the early stage of *P. aeruginosa* biofilm formation by interaction with Fap. It is demonstrate that biofilm in mouse corneal infection model is detected by CDy11 under the stereomicroscopy (Figure 4).

Additionally, in the clinical treatment, biofilm can be formed on the surface of medical instruments such as urinary catheter and implant device. One of main medical materials is silicon which is highly utilized for medical device because it has high chemical resistance, no allergic reaction and very low immune response.³⁰ CDy11 was tested with an implant model which mimicked biofilm forming condition by insertion of biofilm coated silicone tube into peritoneal cavity. The implants were inspected by laser confocal scanning microscopy after removal from the mice. The signal intensity of CDy11 was significantly higher from the silicone tube coated with biofilm than from the noncoated silicone. Furthermore, CDy11 did not stain cellular components adhering to the implant originated from mouse (Supporting Information Figure S7B). Therefore, CDy11 can be applied for detecting biofilms on medical instruments safely with silicone coated artificial joint or medical instruments, because CDy11 showed no background fluorescence when it was tested with in silicone tube implant mouse model.

As mentioned in the Introduction, there are several methods to detect biofilm in vitro but, those are difficult to transfer to in

vivo conditions due to the lack of binding specificity with biofilms.^{9,28} One exception is fluorescence in situ hybridization (FISH), but this requires sample fixing and therefore cannot be used for real-time monitoring.

Planktonic bacteria are easily neutralized by immune systems in vivo, while the matrix encapsulated bacteria are protected against immune systems and antibiotics. Detection of biofilms enables their control and removal. Therefore, there is existing demand for new methods to detect biofilm in vivo with rapid and low cost process and visualization of biofilms with new tools is very important for clinical purpose.

CDy11, developed as a *P. aeruginosa* biofilm imaging probe, will be an option for detecting *P. aeruginosa* biofilm in vivo. For noninvasive tracking of signals to detect biofilm in deeper parts, CDy11 would have to be modified due to the limitation of penetration depth. However, the ability to visualize biofilm forming region in eyes and in implants by CDy11 by invasive tracking of fluorescence signals to biofilm-forming regions will be very useful application.

CONCLUSION

CDy11 was developed as a novel biofilm imaging probe from DOFL and its working mechanism was elucidated by testing putative target of amyloid, through surface plasma resonance assay and antibody costaining. Furthermore, CDy11 was demonstrated as in vivo diagnostic tool for detecting biofilms by testing it in two different animal models, corneal infection model and implant model.

MATERIALS AND METHODS

General Procedure for the Synthesis of CDy11. To a solution of BODIPY Aniline (BDN)²⁹ (*x* equiv) in dry acetonitrile (ACN) was added with corresponding aldehyde (4*x* equiv), followed by pyridine (6*x* equiv) and refluxed at 85 °C for 5 min. The crude condensed BODIPY compound was finally purified by silica gel chromatography in 7:3 hexane and ethyl acetate mixture. The purified compound (0.02 mmol) from the above step was dissolved in dichloromethane (DCM) and added with 100 μL of saturated solution of NaHCO₃, followed by acetyl chloride (5 equiv) at 0 °C. Then the reaction mixture was stirred at room temperature for 30 min. The acetylated compound was purified by silica gel chromatography in 7:3 hexane and ethyl acetate mixture.

Characterization of CDy11. ¹H NMR (CDCl₃, 300 MHz): δ 1.69 (s, 3H), 2.28 (s, 3H), 3.89 (s, 3H), 6.45 (m, 2H), 6.68 (m, 1H), 6.8 (m, 2H), 7 (s, 1H), 7.38 (m, 3H), 7.74 (m, 5H). ¹³C NMR (DMSO-*d*₆, 75 MHz): δ 15.5, 24.5, 56.4, 102.4, 112.1, 116.3, 116.4, 116.7, 118.8, 120.2, 126.4, 127.9, 130.0, 130.1, 130.7, 130.8, 133.6, 134.8, 138.3, 141.1, 142.0, 146.1, 158.0, 162.5, 162.6, 169.1, 174.6. HRMS: *m/z* (C₂₇H₂₂BF₃N₃O₂) calculated: 488.1767, found: 488.1751 (M-H). Extinction coefficient (ε): 12456 M⁻¹ cm⁻¹ (Solvent: Ethanol, Wavelength (λ): 558 nm).

Quantum Yield Measurements. Quantum yield were calculated by measuring the integrated area of emission spectra for CDy11 compound in comparison to the same measurement for Rhodamine B (Φ_{st} = 0.5) as reference compound in ethanol. Both CDy11 and Rhodamine B were excited at 510 nm and emission spectra were collected from 550 to 700 nm.

$$\Phi_x = \Phi_{st}(I_x/I_{st})(A_{st}/A_x)(\eta_x^2/\eta_{st}^2) \quad (1)$$

Quantum yields were calculated using eq 1, Where “Φ_{st}” is the reported quantum yield of the standard, “I” is the integrated emission spectrum, “A” is the absorbance at the excitation wavelength, and “η” is the refractive index of the solvents used. The subscript “x” denotes unknown and “st” denotes standard. Emission was integrated between 550 and 700 nm, and quantum yield for CDy11 was found to be 0.047.

Cell Based Screening for Isolating Primary Hits. *P. aeruginosa* strains used in cell based screening are PAO1 and PAO1Δfap. PAO1 and PAO1Δfap²⁴ strains grown at 37 °C for 20 h in ABTGC media were diluted 1:200 in 10 mL ABTGC media and aliquots were cultured in 96 well microplates (100 μL per well) for 20 h at 37 °C incubator. The next day, 1 μL (100 μM) of compound library dissolved in DMSO was incubated with cultured cells for 1 h before observation of images under EVOS_{fl} microscope (AMG, Mill Creek, WA).

Secondary and Tertiary Screening for Final Hits. PAO1 and PAO1Δfap were cultured in 50 mL conical tube with 2 pieces of cover glass by adding 5 mL ABTGC media (1:200 dilution) at 37 °C incubator without shaking for acquiring biofilm on cover glass. Cover glass was taken and briefly washed with dH₂O for removing planktonic cells before put on slide glass. Subsequently, 5 μL of primary hits (1 μM) was incubated with biofilm for 1 h before taking better resolution of images under fluorescence microscope (Axio Observer Z1; Carl Zeiss).

3D-SIM Super Resolution Images. Precultured *P. aeruginosa* (PAO1-GFP)²⁴ in ABTGC media was inoculated in 8 well chamber plates with 1:200 dilution rates and incubated for 20 h at 37 °C incubator. Next day, 2 μL of 100 μM CDy11 was treated in 200 μL cultured bacteria and incubated in 37 °C incubator for 1 h. All of supernatants were removed before observation of images. Images were taken with ×100 magnification oil lens (Zeiss ELYRA PS.1, Jena, Germany). Images under FITC (Fluorescein isothiocyanate) channel were taken before acquiring images by CDy11 under TRITC channel. Two images taken under different channels were processed to super resolution images and finally merged.

Surface Plasmon Resonance (SPR). Amyloids were prepared in HEPES buffer (0.01 M HEPES, pH 7.4, 0.15 M NaCl, 3 mM EDTA and 0.005% P20). Amyloid fibers were fragmented with sonication at 80 Hz for 10 s and centri futed at 14 000g for 30 s to remove any large fibers. Con-centrate (40 μL) was mixed with 10 mM sodium acetate (120 μL), pH 5.5 right before immobilization.

SPR experiments were performed at 25 °C using Biacore T-200 biosensor with research grade CM5-S sensor chips (Biacore, GE Healthcare). Carboxymethylated CM5-S chips were activated using 70 μL of 0.2 M 1-ethyl-3-[3-(dimethylamino)propyl] carbodiimide hydrochloride (EDC) and 0.05 M *N*-hydroxysuccinimide (NHS) in a 1:1 ratio. Amyloid in sodium acetate solution (100 μL) was injected over the activated surface until an immobilization level of 7700 response units (RU) was reached. Ethanolamine hydrochloride (1.0 M), pH 8.5 was injected across the surface for 5 min to block any residual activated-unreacted carboxyl groups. Compounds were dissolved into HEPES buffer containing final concentration of 5% DMSO and serially diluted to 340 nM, 1.03, 3.09, 9.26, 27.78, 83.33 μM. Tht+ was prepared similarly as positive control. Replicates of the diluted compounds were injected across an unmodified flow cell and amyloid-immobilized flow cell in a serial manner for association phase of 60 s followed by dissociation phase of 5 min. Regeneration was not performed since all compounds exhibit complete dissociation within the dissociation duration. The chip surface was rinsed using HEPES buffer. All sensorgrams were double-referenced with responses from unmodified channel and blank HEPES buffer injections. Equilibrium responses from the compounds were plotted against logarithmic of their corresponding concentrations where the binding affinities were calculated from 50% saturation.

Generation of Eye Infection Model. *P. aeruginosa* (PAO1-GFP) was grown at 37 °C in ABTGC media for 16 h. 500 μL of cultured PAO1-GFP was transferred to 1.5 mL eppendorf tube and centrifuged at 14 000g for 3 min. Supernatant was removed and pellet was washed with PBS buffer 3 times. Finally, pellet was resuspended in 250 μL of PBS buffer.

Mice were anesthetized ketamine/xylazine by peritoneal injection before scratches were made in cornea with blade. PAO1-GFP (1 μL, 2 × 10⁷ ~ 10⁸ CFU) dissolved in PBS buffer was treated in left eye and PBS buffer was treated in right eye. *P. aeruginosa* inoculated mice were incubated for 2 days before in vivo experiments. Animal handling was in accordance with the Institutional Animal Care and Use Committee

of Singapore Bioimaging Consortium (Agency of Science, Technology and Research, Singapore).

Immunohistochemistry. Rabbit polyclonal antisera targeting *P. aeruginosa* Fap was obtained from BioGenes (Berlin, Germany). Briefly, rabbits were immunized with 100 μ g of purified FapC monomers²¹ at day 0 and again after 7, 14, 28, and 70 days. The rabbits were sacrificed after 77 days and antisera collected. The antisera showed an ELISA titer of >1:200 000 against purified FapC compared to a titer of 1:300 for the corresponding preimmune sera.

The OCT freezing media embedded sections were cleared by incubating with 1% gelatin PBS buffer for 30 min and remaining solution was removed before incubating with Fap anti-immune serum solution in 1% gelatin PBS buffer for 2 h at 37 °C. Samples were washed 3 times with 400 μ L washing buffer (1% gelatin, 0.1% triton \times 100 in PBS) before incubating with secondary antibody linked with Cy5 fluorophore for 1 h at 37 °C. Finally, samples were examined with fluorescent microscope after 3 times washing with washing buffer (2.5% tween 20 in PBS).

Preparation of Bacterial Coating Implant. One bacterial colony (PAO1-GFP) was picked up from the plate to inoculate an overnight culture in LB (Luria Broth) media in 37 °C incubator with 110 rpm/min for 20 h. Silicone tubes (Ole Dich) were cut with a thickness of 4 mm and were sterilized in 0.5% NaClO for overnight. Next day, 25 mL of overnight cultured media was transferred to 50 mL conical tube and pellet was collected by centrifuging at 3000 rpm for 10 min. Subsequently, pellet was suspended with 2 mL of LB media before optical density was observed under 600 nm wavelength.

Sterilized silicone was washed twice in 0.9% NaCl solution. Silicone tubes (8 pieces) in 50 mL flask were incubated with 10 mL of diluted bacteria (OD₆₀₀ = 0.1) in 0.9% NaCl solution in rotary shaker at 37 °C with 110 rpm/min for 20 h.

Generation of Implant Model. After anesthesia of mice with ketamine/xylazine mix by intraperitoneal injection, the mouse was placed ventral side up on plate. Fur was clipped and the skin was swabbed with 70% ethanol. An incision of approximately 0.5–1 cm was made in the left groin area. Then an implant prepared the day before was inserted into peritoneal cavity via the incision. The incision was closed with a suture and healed on warm pad at 26–28 °C.

■ ASSOCIATED CONTENT

Supporting Information

The Supporting Information is available free of charge on the ACS Publications website at DOI: 10.1021/jacs.5b11357.

Detailed synthetic procedure and building block structures with characterization. (PDF)

■ AUTHOR INFORMATION

Corresponding Author

*chmcyt@nus.edu.sg

Notes

The authors declare the following competing financial interest(s): J.-Y.K., S.S., M.G., L.Y., and Y.-T.C. are the inventors of CDy11 for which a patent has been applied.

■ ACKNOWLEDGMENTS

The authors would like to acknowledge financial support from the Singapore Centre on Environmental Life Sciences Engineering (SCELSE), whose research is supported by the National Research Foundation Singapore, Ministry of Education, Nanyang Technological University and National University of Singapore, under its Research Centre of Excellence Programme.

■ REFERENCES

- (1) Stubbings, W.; Labischinski, H. *F1000 Biol. Rep.* **2009**, *1*, 40.
- (2) Fröls, S. *Biochem. Soc. Trans.* **2013**, *41*, 393.
- (3) Donlan, R. M. *Emerging Infect. Dis.* **2002**, *8*, 881.
- (4) Alhede, M.; Bjarnsholt, T.; Givskov, M.; Alhede, M. *Adv. Appl. Microbiol.* **2014**, *86*, 1.
- (5) Alhede, M.; Bjarnsholt, T.; Jensen, P. Ø.; Phipps, R. K.; Moser, C.; Christophersen, L.; Christensen, L. D.; van Gennip, M.; Parsek, M.; Høiby, N.; Rasmussen, T. B.; Givskov, M. *Microbiology* **2009**, *155* (11), 3500.
- (6) *Immunology of Biofilms* (PA-07-288); NIH, Department of Health and Human Services, 2007-01-09.
- (7) *Research on Microbial Biofilms* (PA-03-047); NIH, National Heart, Lung, and Blood Institute, 2002-12-20.
- (8) Li, L.; Mendis, N.; Trigui, H.; Oliver, J. D.; Faucher, S. P. *Front. Microbiol.* **2014**, *5*, 258.
- (9) Trachoo, N. *Songklanakarini J. Sci. Technol.* **2003**, *25*, 807.
- (10) Ma, L.; Lu, H.; Sprinkle, A.; Parsek, M. R.; Wozniak, D. J. *J. Bacteriol.* **2007**, *189*, 8353.
- (11) Anastasiadis, P.; Mojica, K. D.; Allen, J. S.; Matter, M. L. *J. Nanobiotechnol.* **2014**, *12*, 24.
- (12) Im, C. N.; Kang, N. Y.; Ha, H. H.; Bi, X.; Lee, J. J.; Park, S. J.; Lee, S. Y.; Vendrell, M.; Kim, Y. K.; Lee, J. S.; Li, J.; Ahn, Y. H.; Feng, B.; Ng, H. H.; Yun, S. W.; Chang, Y. T. *Angew. Chem., Int. Ed.* **2010**, *49*, 7497.
- (13) Lee, J. S.; Kang, N. Y.; Kim, Y. K.; Samanta, A.; Feng, S.; Kim, H. K.; Vendrell, M.; Park, J. H.; Chang, Y. T. *J. Am. Chem. Soc.* **2009**, *131*, 10077.
- (14) Agrawalla, B. K.; Chandran, Y.; Phue, W. H.; Lee, S. C.; Jeong, Y. M.; Wan, S. Y.; Kang, N. Y.; Chang, Y. T. *J. Am. Chem. Soc.* **2015**, *137*, 5355.
- (15) Kang, N. Y.; Lee, S. C.; Park, S. J.; Ha, H. H.; Yun, S. W.; Kostromina, E.; Gustavsson, N.; Ali, Y.; Chandran, Y.; Chun, H. S.; Bae, M. A.; Ahn, J. H.; Han, W.; Radda, G. K.; Chang, Y. T. *Angew. Chem., Int. Ed.* **2013**, *52*, 8557.
- (16) Er, J. C.; Leong, C.; Teoh, C. L.; Yuan, Q.; Merchant, P.; Dunn, M.; Sulzer, D.; Sames, D.; Bhinge, A.; Kim, D.; Kim, S. M.; Yoon, M. H.; Stanton, L. W.; Je, S. H.; Yun, S. W.; Chang, Y. T. *Angew. Chem., Int. Ed.* **2015**, *54*, 2442.
- (17) Kang, N. Y.; Ha, H. H.; Yun, S. W.; Yu, Y. H.; Chang, Y. T. *Chem. Soc. Rev.* **2011**, *40*, 3613.
- (18) Ramsey, D. M.; Wozniak, D. J. *Mol. Microbiol.* **2005**, *56*, 309.
- (19) Nickel, J. C.; Ruseska, I.; Wright, J. B.; Costerton, J. W. *Antimicrob. Agents Chemother.* **1985**, *27*, 619.
- (20) Robertson, D. M.; Cavanagh, H. D. *Clin. Ophthalmol.* **2008**, *2*, 907.
- (21) Seviour, T.; Hansen, S. H.; Yang, L.; Yau, Y. H.; Wang, V. B.; Stenvang, M. R.; Christiansen, G.; Marsili, E.; Givskov, M.; Chen, Y. J. *J. Biol. Chem.* **2015**, *290*, 6457.
- (22) Zeng, G.; Vad, B. S.; Dueholm, M. S.; Christiansen, G.; Nilsson, M.; Tolker-Nielsen, T.; Nielsen, P. H.; Meyer, R. L.; Otzen, D. E. *Front. Microbiol.* **2015**, *6*, 1099.
- (23) Herbst, F.-A.; Søndergaard, M. T.; Kjeldal, H.; Stensballe, A.; Nielsen, P. H.; Dueholm, M. S. *J. Proteome Res.* **2014**, *14*, 72.
- (24) Dueholm, M. S.; Søndergaard, M. T.; Nilsson, M.; Christiansen, G.; Stensballe, A.; Overgaard, M. T.; Givskov, M.; Tolker-Nielsen, T.; Otzen, D. E.; Nielsen, P. H. *MicrobiologyOpen* **2013**, *2*, 365.
- (25) Girgis, D. O.; Sloop, G. D.; Reed, J. M.; O'Callaghan, R. J. *Invest. Ophthalmol. Visual Sci.* **2003**, *44*, 1591.
- (26) Bjarnsholt, T.; Gennip, M. V.; Jakobsen, T. H.; Christensen, L. D.; Jensen, P. Ø.; Givskov, M. *Nat. Protoc.* **2010**, *5*, 282.
- (27) George, A. O. *J. Vis. Exp.* **2011**, *47*, 2437.
- (28) Kang, N. Y.; Lee, S. C.; Park, S. J.; Ha, H. H.; Yun, S. W.; Kostromina, E.; Gustavsson, N.; Ali, Y.; Chandran, Y.; Chun, H. S.; Bae, M.; Ahn, J. H.; Han, W.; Radda, G. K.; Chang, Y. T. *Angew. Chem., Int. Ed.* **2013**, *52*, 8557.
- (29) Brouwer, A. M. *Pure Appl. Chem.* **2011**, *83*, 2213.
- (30) Lawrence, E. L.; Turner, I. G. *Med. Eng. Phys.* **2005**, *27*, 443.